Developmental Cell
Article

Phactr4 Regulates Neural Tube and Optic Fissure Closure by Controlling PP1-, Rb-, and E2F1-Regulated Cell-Cycle Progression

Tae-Hee Kim,[1,2,3] Jessica Goodman,[3] Kathryn V. Anderson,[1,2] and Lee Niswander[1,3,*]
[1] Cell Biology and Genetics Program, Weill Graduate School of Medical Sciences of Cornell University, New York, NY 10021, USA
[2] Developmental Biology Program, Sloan-Kettering Institute, New York, NY 10021, USA
[3] Howard Hughes Medical Institute, Department of Pediatrics, Section of Developmental Biology, University of Colorado at Denver, and Health Sciences Center, Aurora, CO 80045, USA
*Correspondence: lee.niswander@uchsc.edu
DOI 10.1016/j.devcel.2007.04.018

SUMMARY

Here we identify the *humpty dumpty* (*humdy*) mouse mutant with failure to close the neural tube and optic fissure, causing exencephaly and retinal coloboma, common birth defects. The *humdy* mutation disrupts Phactr4, an uncharacterized protein phosphatase 1 (PP1) and actin regulator family member, and the missense mutation specifically disrupts binding to PP1. *Phactr4* is initially expressed in the ventral cranial neural tube, a region of regulated proliferation, and after neural closure throughout the dorsoventral axis. *humdy* embryos display elevated proliferation and abnormally phosphorylated, inactive PP1, resulting in Rb hyperphosphorylation, derepression of E2F targets, and abnormal cell-cycle progression. Exencephaly, coloboma, and abnormal proliferation in *humdy* embryos are rescued by loss of *E2f1*, demonstrating the cell cycle is the key target controlled by Phactr4. Thus, Phactr4 is critical for the spatially and temporally regulated transition in proliferation through differential regulation of PP1 and the cell cycle during neurulation and eye development.

INTRODUCTION

Neurulation is a fundamental morphogenetic process during vertebrate embryogenesis whereby the neural plate rolls up to form the neural tube, the embryonic precursor of the central nervous system (Colas and Schoenwolf, 2001). Defects in neural tube closure occur in ~1 in 1000 human births, making it the second most common birth defect (Juriloff and Harris, 2000). Cranial region neural tube defects are called anencephaly in humans and exencephaly in mice, and spinal cord neural tube defects are called spina bifida. The high incidence of neural tube closure defects reflects the complexity of the process in which there must be tight coordination of proliferation and differentiation, patterning, cell death, cell-shape changes, and cell movement. These events must also be coordinated between the neural tissue and neighboring ectoderm and mesenchyme (Copp et al., 2003).

At the time of normal cranial neural closure, there is regulated proliferation along the dorsal and ventral axis of the neural tube, with more proliferation in the dorsal versus the ventral half (Copp et al., 2003). Following neural closure, proliferation is more uniform along the dorsoventral aspect of the cranial neural tube, but this early difference in dorsoventral proliferation is now evidenced by a greater number of differentiated cells in the ventral neural tube. Although it has been speculated that early spatially regulated proliferation is critical for proper neural tube closure and differential proliferation is important in regulating the timing of neuronal differentiation, it is unclear what genes are required to achieve this regulation during development or the fundamental importance of this regulation in neural closure.

Although no genes have been identified which control the dorsoventrally regulated proliferation, some mouse mutants display exencephaly due to excessive cell proliferation throughout the neural tissue. Overexpression of Notch3 results in an increased number of neuronal progenitors and exencephaly (Lardelli et al., 1996). Mutations in tumor suppressor genes can cause abnormal neural proliferation and exencephaly, including a subset of *p53*-deficient embryos (Sah et al., 1995) and a hypomorphic mutation in *brca1* (Gowen et al., 1996). Heterozygotes of the chromatin remodeling complex, such as Brg1 and Srg1, are predisposed to exencephaly and tumors of the nervous system (Kim et al., 2001).

A number of protein kinases have been identified as key regulators of cell-cycle progression, and specific phosphatases counter their activity (Berndt, 2003). Protein phosphatase 1 (PP1) is a major serine/threonine phosphatase that regulates a variety of cellular functions through interactions with more than 50 different targeting subunits (Cohen, 2002). PP1 function in the cell cycle is best understood through its regulation of the retinoblastoma protein Rb. In vitro studies show the catalytic subunit of PP1

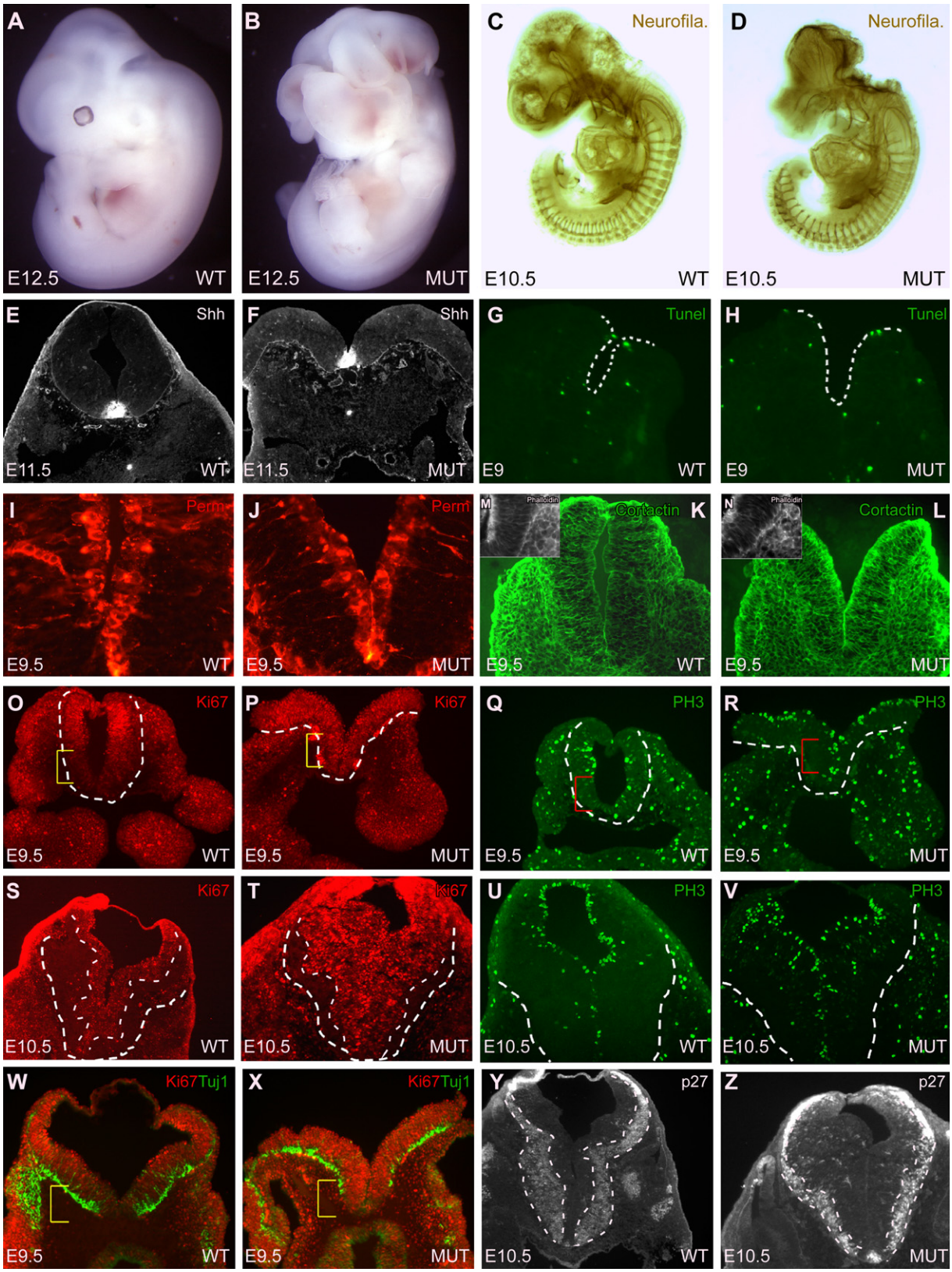

Figure 1. Increased Proliferation and Reduced Differentiation in *humdy* Neural Tube
(A and B) Lateral views of E12.5 wild-type (WT) and *humdy* (MUT) exencephalic embryos.
(C and D) Whole-mount antineurofilament antibody staining.

interacts with and dephosphorylates Rb, leading to Rb activation (Durfee et al., 1993; Tamrakar et al., 2000; Vietri et al., 2006). Hypophosphorylated Rb binds to and sequesters E2F transcription factors, inhibiting transcription of genes required for the G1/S transition and thus inhibiting cell-cycle progression. As cells progress through late G1 and S phase, Rb becomes hyperphosphorylated and inactivated by cyclin/cdk complexes (Pagano and Jackson, 2004; Sherr and Roberts, 2004), leading to release of E2F and transcription of E2F targets required for cell-cycle progression. Therefore, regulation of Rb phosphorylation is critical in cell-cycle control. Genetic studies have shown PP1 is required for progression through or exit from mitosis in *Aspergillus nidulans* (Doonan and Morris, 1989), fission yeast (Booher et al., 1989; Ohkura et al., 1989), and *Drosophila* (Axton et al., 1990). Because Rb is thought to be a target of PP1, one important mechanism of PP1-mediated mitotic exit may involve activation of G1-specific regulators such as Rb. Treatment of mitotic cell extracts with PP1-specific inhibitors inhibits Rb dephosphorylation (Ludlow et al., 1993). PP1 regulation of Rb is controlled by an inhibitory phosphorylation on threonine 320 of PP1 that is observed during M phase and in late G1 through early S (Liu et al., 1999b). A constitutively active T320A mutant of PP1, but not wild-type PP1, retains Rb in a hypophosphorylated and activated state and causes cell-cycle arrest at G1/S transition. Furthermore, T320A PP1 mutant does not impede cell-cycle progression in *Rb*-negative cells, indicating PP1 requires functional Rb to induce growth arrest (Berndt et al., 1997). This suggests inactivation of PP1 sometime during G1 is required to allow Rb phosphorylation and initiation of S phase. However, in vivo genetic evidence for PP1 regulation of Rb during the cell cycle is still missing. Moreover, an understanding of PP1 functions in vivo has remained elusive and is complex, as PP1 regulates many different biological processes and there are three genes that encode the three forms of PP1 (α, β, γ) in mammals.

To better understand PP1 function, a yeast two-hybrid screen was performed to identify PP1α-interacting proteins (Allen et al., 2004). A novel protein strongly expressed in brain was identified with PP1- and actin-binding domains at the C terminus, and named phosphatase and actin regulator 1 (Phactr1). By sequence homology, three other family members were identified (called *Phactr2–4*). Although Phactr family proteins lack a consensus PP1-binding sequence (R/K-R/K-hydrophobic-X-F/W) defined in other PP1-binding proteins, all four members show strong conservation of their own PP1- and actin-binding domains (Allen et al., 2004). However, the functional relevance of this binding has not been established and the in vivo functions of the Phactr family members are not known.

Although the cellular events during neurulation are well documented, the mechanisms controlling this complex process are poorly understood. To gain a better understanding of the genes involved in neurulation and the mechanisms by which they act, we have undertaken forward genetic screens in mice to identify mutations that affect neural tube closure (Kasarskis et al., 1998; Zohn et al., 2005). Following treatment with the chemical mutagen ethyl nitrosourea (ENU) and screening for recessive mutations that affect embryonic neural tube closure, we identified a number of genes of which little is known as to their mechanism of action and which have not been implicated in neural development. Here we describe the *humdy* mouse mutant with defects in closure of the neural tube and optic fissure. The *humdy* gene encodes Phactr4, an uncharacterized member of the Phactr family. A missense mutation was found in the proposed PP1-binding domain, and this specifically disrupts binding of PP1 to Phactr4. This leads to an increase in T320 inhibitory phosphorylation on PP1 in the ventral neural tube and eye and disruption of PP1 activity toward its target Rb. This causes Rb to become hyperphosphorylated and inactivated, leading to derepression of E2F targets. Loss of Phactr4 function results in shortening of the cell cycle, an increase in proliferating neural progenitors, and ectopic cell division and/or cell-cycle exit defects in differentiating cells of the *humdy* neural tube and retina. To demonstrate that the key target of Phactr4/PP1 is the cell cycle, we generated embryos mutant for both *phactr4*$^{humdy/humdy}$ and *E2f1*. Loss of *E2f1*, even loss of a single allele, results in rescue of exencephaly, coloboma, and proliferation/differentiation defects, providing strong genetic and functional evidence that the critical target of Phactr4 is the cell-cycle regulator E2F1. Thus, our studies identify a critically required pathway from Phactr4 to the in vivo regulation of PP1 and Rb activity to E2F1 in cell-cycle control which is necessary for proper neural tube closure and eye development.

RESULTS

humdy Mutant Mouse Embryos Display Neural Tube and Eye Defects

To study neurulation in an unbiased way, we performed ENU mutagenesis screens for recessive mutations in mice which cause neural tube closure defects (NTD) (Kasarskis et al., 1998; Zohn et al., 2005). From this screen, we isolated the *humpty dumpty* (*humdy*) mutant mouse line that displays extensive cranial neurulation and eye defects (Figures 1A–1D and 2A–2H). To

(E–V) Cross-sections of wild-type and *humdy* cranial neural tube detected for Shh protein in the floor plate (E and F); TUNEL staining for apoptotic cells (G and H); phospho-ERM, cortactin, and phalloidin (I–N); and proliferation markers Ki67 ([O, P, S, and T]; late G1-M phase) and PH3 ([Q, R, U, and V]; M phase).

(W–Z) The neuronal differentiation marker TuJ1 (green in [W] and [X]; Ki67, red) and cell-cycle inhibitor p27 (Y and Z) show reduced differentiation in *humdy* neural tube. Brackets indicate ventral side of neural tube, dotted lines outline the neural tube, and double dotted lines in (S), (T), (Y), and (Z) highlight differentiated cells. Embryonic age is indicated in each panel.

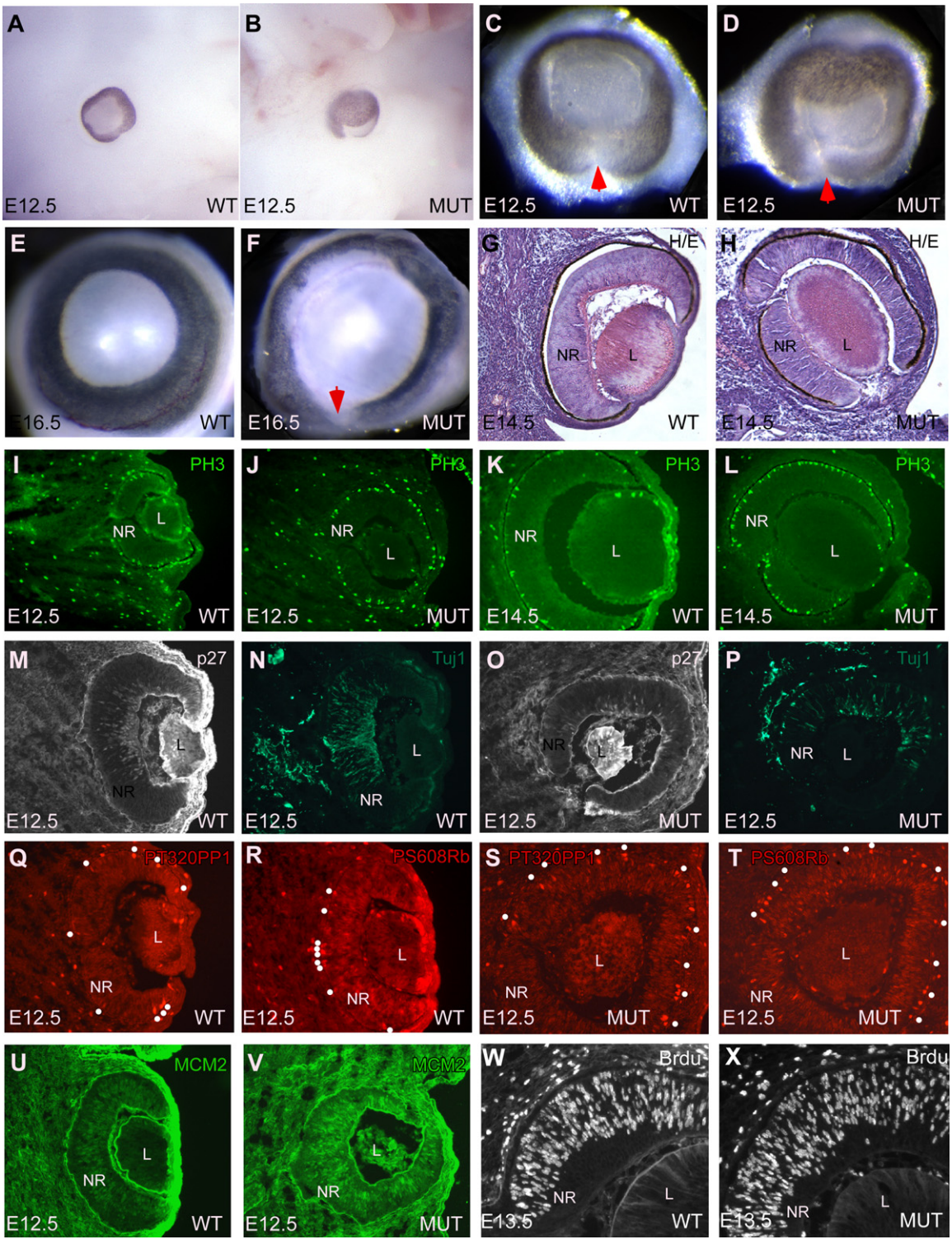

Figure 2. Increased Proliferation and Abnormal PP1 and Rb Phosphorylation in *humdy* Retina

(A–H) Wild-type (WT) and *humdy* (MUT) eye showing expanded retinal pigment epithelium (B, D, and H) and retinal coloboma ([D and F], red arrow) in *humdy* eye.

(G and H) Histology of eye in cross-section from wild-type and *humdy* E14.5 embryos showing retina overgrowth.

(I–X) Cross-sections of wild-type and *humdy* eye detected with proliferation marker PH3 ([I–L], green; M phase), cell-cycle inhibitor p27 (M and O), and neuronal differentiation marker TuJ1 ([N and P], green) showing increased proliferation and reduced differentiation in *humdy* retina.

(Q and S) Anti-PT320PP1 antibody shows increased number of cells with inactive PP1 in *humdy* eye.

characterize the general morphological defects, embryos were examined from embryonic day (E) 8.5 to E16.5. By E9.25, mutant embryos can be distinguished by their failure to close the cranial neural tube. About 15% of *humdy* homozygous mutant embryos exhibit severe exencephaly, along with a wavy spinal neural tube and a shortened anterior/posterior body axis, and they die around E10.5 (data not shown). The remaining homozygous mutant embryos exhibit complete exencephaly from the forebrain to hindbrain (Figures 1A and 1B). Most *humdy* embryos die by E14.5, but a few survive to birth and die shortly thereafter. Approximately 8% (7/93) of heterozygous embryos display a midbrain region-specific exencephaly (data not shown), indicating an incompletely penetrant dominant effect.

humdy embryos also have eye defects. Homozygous mutant embryos display overgrowth of the neural retina and retinal pigment epithelium (RPE) (Figures 2A–2D, 2G, and 2H). The primordium of the eye initiates from the neuroepithelium of the ventral diencephalon. It evaginates to form optic vesicles and subsequently invaginates to form the optic cup. The point at which the laterally growing edges of the optic cup fuse is called the optic fissure (Chow and Lang, 2001). Failure of optic fissure closure can lead to coloboma, which occurs in 1 in 10,000 human births (Weston et al., 2003). *humdy* embryos also display coloboma at E12.5 and E16.5 (Figures 2C–2F).

Increased Proliferation and Decreased Differentiation in *humdy* Neural Tube and Retina

To distinguish the underlying cause of exencephaly, we used molecular markers to examine a number of cellular events during neurulation. Patterning and apoptosis were not obviously altered in *humdy* mutant neural tube (E8.5–E11.5) or retina (E12.5) (Figures 1C–1H; see Figures S1 and S2 in the Supplemental Data available with this article online). There was no apparent change in cytoskeletal architecture, cell morphology, neuroepithelial integrity, or actin localization in the *humdy* neural tube (Figures 1I–1N; phospho-ERM, cortactin, phalloidin staining). There was no defect in medial hinge point formation, and dorsolateral hinge point formation was inconsistently affected, with some samples showing a defect and others no defect (e.g., Figure 1P and 6B, respectively).

Overgrowth of brain tissue, neural retina, and RPE suggested proliferation is disrupted in *humdy* neural tube and eye. Proliferation in the presumptive mid-/hindbrain region was first analyzed with Ki67 antibody, a late G1-M phase marker. At E9.5, in wild-type embryos during cranial neural closure there is spatially regulated proliferation, with more proliferation in the dorsal than ventral neural tube (Figure 1O). In the *humdy* cranial neural tube, however, this regulation was disrupted with greatly increased proliferation ventrally (Figure 1P), more similar to proliferation normally seen dorsally. In wild-type embryos at E10.5 after neurulation, proliferation is more uniform along the dorsoventral axis (Figure 1S). In E10.5 *humdy* cranial neural tube, the number of Ki67-positive cells was greatly increased both ventrally and dorsally (Figure 1T). Examination of cells in M phase using an anti-phospho-histone H3 (PH3) antibody also showed abnormal proliferation in the *humdy* ventral neural tube at E9.5 and then in both the dorsal and ventral regions at E10.5 (Figures 1Q, 1R, 1U, and 1V). The number of mitotic cells was quantified (see Experimental Procedures) and found to be increased ~2-fold (statistically significant; p value = 0.046) in the E9.5 *humdy* ventral neural tube. Moreover, at this stage there was no longer a significant difference in proliferation between the dorsal and ventral regions.

As differentiation is tightly linked to exit from the cell cycle, two markers of neuronal differentiation, TuJ1 and p27, a cell-cycle inhibitor, were examined. Starting by E9.5 in the wild-type cranial neural tube, proliferating neuronal progenitors in the ventricular zone begin to exit the cell cycle, differentiate, and migrate laterally (Figures 1W and 1Y). This pattern of differentiation is particularly evident in the ventral neural tube both at E9.5 and E10.5 and correlates with the domain of reduced proliferation at E9.5. In the *humdy* cranial neural tube at E9.5 and E10.5, abnormal differentiation was observed as the number of TuJ1- and p27-positive cells were reduced, particularly in the ventral half (Figures 1X and 1Z), corresponding to the region of abnormal proliferation.

Defects in morphogenesis of the *humdy* eye were also related to increased proliferation and decreased differentiation. At E12.5 and E14.5, there were significantly more PH3-positive mitotic cells (Figures 2I–2L; average difference between wild-type and mutant retina is 4.8; p = 0.042) and fewer p27-positive cells and differentiated neurons (Figures 2M–2P) in the *humdy* neural retina compared to wild-type. Taken together, this indicates the neural tube and retinal defects in *humdy* mutant embryos are due to misregulation of proliferation and differentiation. Cranial neural tube closure normally occurs by E8.5–E9.5 at the time of spatially restricted proliferation along the dorsoventral axis. *humdy* NTD is associated with locally deregulated proliferation in the ventral aspect of the neural tube. Although this differential proliferation has been noted previously, the *humdy* mutant provides evidence that this regulated proliferation is necessary for cranial neural tube closure.

Decreased Cell-Cycle Length and Disrupted Cell-Cycle Exit in *humdy* Mutants

To explore further the defects in cell proliferation and differentiation, we quantified the number of progenitor to differentiated cells using anti-Sox9 and -p27 antibodies, respectively. This showed a >2-fold increase in the ratio of proliferating neural progenitors to differentiated cells in the *humdy* hindbrain region (Figures 3A–3C). Conversely,

(R and T) Anti-S608Rb antibody shows increased number of cells with inactive Rb in *humdy* eye. White dots in (Q)–(T) mark neural progenitor cells with inactive PP1 or phosphorylated Rb.

(U–X) Wild-type and *humdy* eyes detected with anti-MCM2 (U and V) or anti-BrdU (W and X) antibodies.

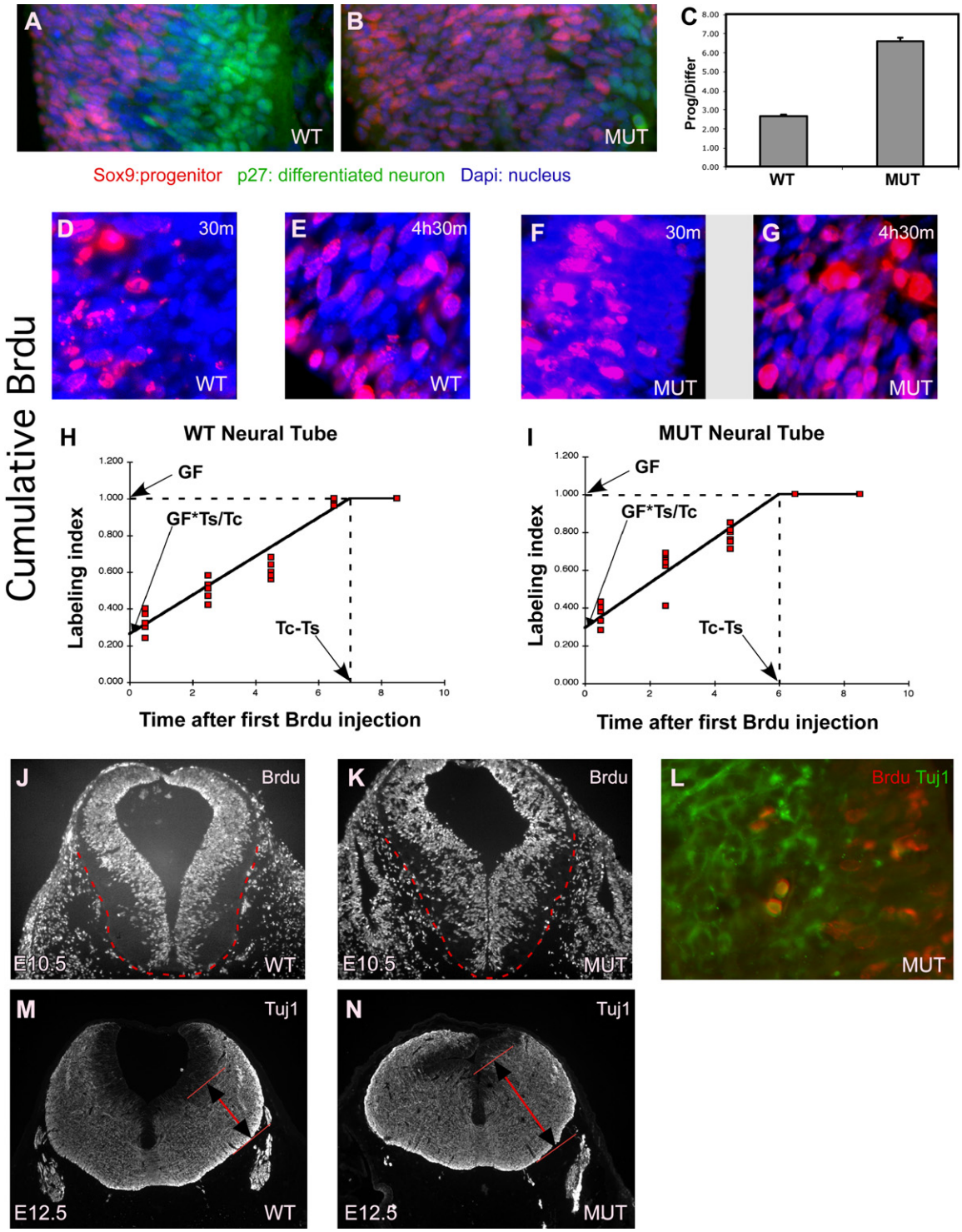

Figure 3. Shortened Cell Cycle and Cell-Cycle Exit Defects in *humdy* Neural Tube

(A and B) Sox9-positive neural progenitors (pink) are increased and p27-positive differentiated neurons (green) are reduced in *humdy* neural tube at E10.5.

(C) Quantification of the ratio of progenitors to differentiated neurons.

(D–I) Cumulative BrdU labeling shows shortening of neural progenitor cell cycle in *humdy* embryos at E10.5. (D–G) BrdU labeling of neural progenitors (red) after indicated time of incubation.

(J–L) BrdU labeling and TuJ1 staining show cell-cycle exit defects and/or abnormal cell-cycle entrance in *humdy* embryos.

(M and N) TuJ1-positive neurons are increased in number in E12.5 *humdy* embryos. Wild-type (WT) and *humdy* (MUT).

there was a decreased number of neurons that expressed markers of differentiation (Figures 1W–1Z and 3A–3C; eye, Figures 2M–2P), indicating a defect in differentiation, and subsequently this leads to significantly increased neurogenesis (Figures 3M and 3N).

To determine whether the increase in number of neural progenitors is related to a change in cell-cycle length, we performed cumulative BrdU incorporation studies. This showed the total cell-cycle length minus S phase length (Tc − Ts) was 7 hr in the wild-type E10.5 cranial neural tube, whereas it was shortened to 6 hr in *humdy* mutants (Figures 3D–3I). Thus, the *Humdy* gene is critical in regulating the pace of the cell cycle within neural progenitors.

We also found the *humdy* mutation affects cell-cycle exit. BrdU labeling showed proliferating cells within the domains of differentiated cells in *humdy* neural tube and retina (Figures 2W, 2X, 3J, and 3K). This ectopic cell division was also shown by coexpression of an early marker of differentiated neurons (TuJ1) and a proliferation marker (BrdU; Figure 3L). Thus, some mutant cells which have turned on markers of differentiated neurons and moved out of the proliferative zone reenter the cell cycle and/or do not properly exit the cell cycle. The shortened cell cycle, increase in number of neural progenitors, and ectopic cell division indicate the *Humdy* gene is critically required in regulation of cell-cycle length and cell-cycle exit.

The *Humdy* Gene Encodes Phactr4, an Uncharacterized Phosphatase and Actin Regulator Protein

The *humdy* mutation was mapped to a 2 Mb region on mouse chromosome 4 using strain-specific polymorphisms and meiotic recombination mapping (Figure 4A). In the region was an annotated but functionally uncharacterized gene called *Phactr4*. Phactr4 is related by sequence homology to Phactr1, which was identified by its interaction with PP1 and actin (Allen et al., 2004). As PP1 plays a role in regulating proliferation, Phactr4 was a good candidate for a regulator of embryonic proliferation. cDNAs of *Phactr4* from wild-type and *humdy* mutant embryos were isolated and sequenced. This identified a missense mutation which changes arginine (Arg) at amino acid 650 to proline (Pro) in the conserved C-terminal region (Figure 4B; Figure S3). To confirm the *Phactr4* mutation is responsible for the *humdy* phenotype, we obtained a second allele of *Phactr4*. BayGenomics embryonic stem cell clone RRA075 contains a gene-trap insertion in the second intron, resulting in fusion of the first five amino acids of Phactr4 in-frame with a β-galactosidase and neomycin phosphotransferase cassette. In a complementation cross, embryos transheterozygous for the *humdy* and gene-trap alleles display exencephaly (Figure 4C), confirming *Phactr4* identification. However, homozygous gene-trap allele embryos often have less severe phenotypes than *humdy* embryos, and indeed we detect some residual Phactr4 protein in sections of *Phactr4* gene-trap mutant embryos (data not shown).

Phactr4 Interacts with PP1 and Actin, and the Missense Mutation in *humdy* Disrupts PP1 Binding

Phactr1, the first member of this family, was identified in a yeast two-hybrid screen by its interaction with PPIα and actin, and these binding sites mapped to the C terminus (Allen et al., 2004). However, the functional significance of this interaction with PP1 is unknown or whether it affects PP1 activity. Phactr4 displays a high level of amino acid sequence homology to Phactr1, especially in the C terminus (Figure S3). Moreover, the *humdy* point mutation is within the proposed PP1-binding domain. We generated a polyclonal antibody to Phactr4 and showed the amino acid change does not affect stability or localization of Phactr4^{humdy} protein in mutant embryos (Figures 5J and 5M). To determine whether mouse Phactr4 interacts with PP1 and whether the point mutation specifically disrupts PP1 binding, we first tested binding in a yeast two-hybrid assay. The *humdy* mutant construct interacted much more weakly with PP1α than wild-type Phactr4 (Figure 4D). We then tested interaction with PP1 and determined whether actin binding was affected by coimmunoprecipitation of endogenous PP1 and actin with Myc-tagged wild-type or *humdy* mutant Phactr4 constructs expressed in 293T cells (Figures 4E and 4F). This showed Phactr4^{humdy} binds actin similarly to wild-type Phactr4 (Figure 4E). Wild-type Phactr4 strongly binds PP1α; however, the Phactr4^{humdy} mutation dramatically disrupts PP1α binding, even in this overexpression assay (Figure 4F). Reciprocal coimmunoprecipitation using anti-PP1α to pull down Phact4 also showed severely disrupted interaction (Figure 4F). Possible interactions of the Phactr family with other PP1 family members have not been tested. Figure 4F shows Phactr4 interacts with PP1β (also called δ) and PP1γ, and these interactions are also significantly reduced by the *humdy* mutation. Thus, the ENU-induced *humdy* mutation results in a unique allele, generating a stable protein with a specific defect in PP1 binding.

Phactr4 Is Expressed in Neural Tube and Retina

To determine whether *Phactr4* is expressed in a pattern consistent with regulation of neural and eye development, *Phactr4* RNA expression was assessed during embryonic development (E8.5–E10.5) using both a digoxygenin-labeled *Phactr4* antisense probe (Figures 5C–5F) and whole-mount *LacZ* staining to detect the gene-trap allele (Figures 5A and 5B). *Phactr4* is most strongly expressed in neural tissue (Figures 5A–5C). Interestingly, and in accordance with the *humdy* phenotype, *Phactr4* is expressed in a dynamic pattern during neurulation. From E8.5 to E9.5, the period of cranial neural closure and spatially regulated proliferation, *Phactr4* is expressed strongly in the ventral region of the cranial neural tube (Figure 5D), the region of abnormal proliferation in *humdy* mutants (Figures 1O and 1P). By E10.5, *Phactr4* is expressed more uniformly along the dorsal and ventral aspects of the cranial neural tube (Figure 5E), the time when ectopic proliferation is observed throughout the dorsoventral aspect of the *humdy* neural tube (Figures 1S and 1T).

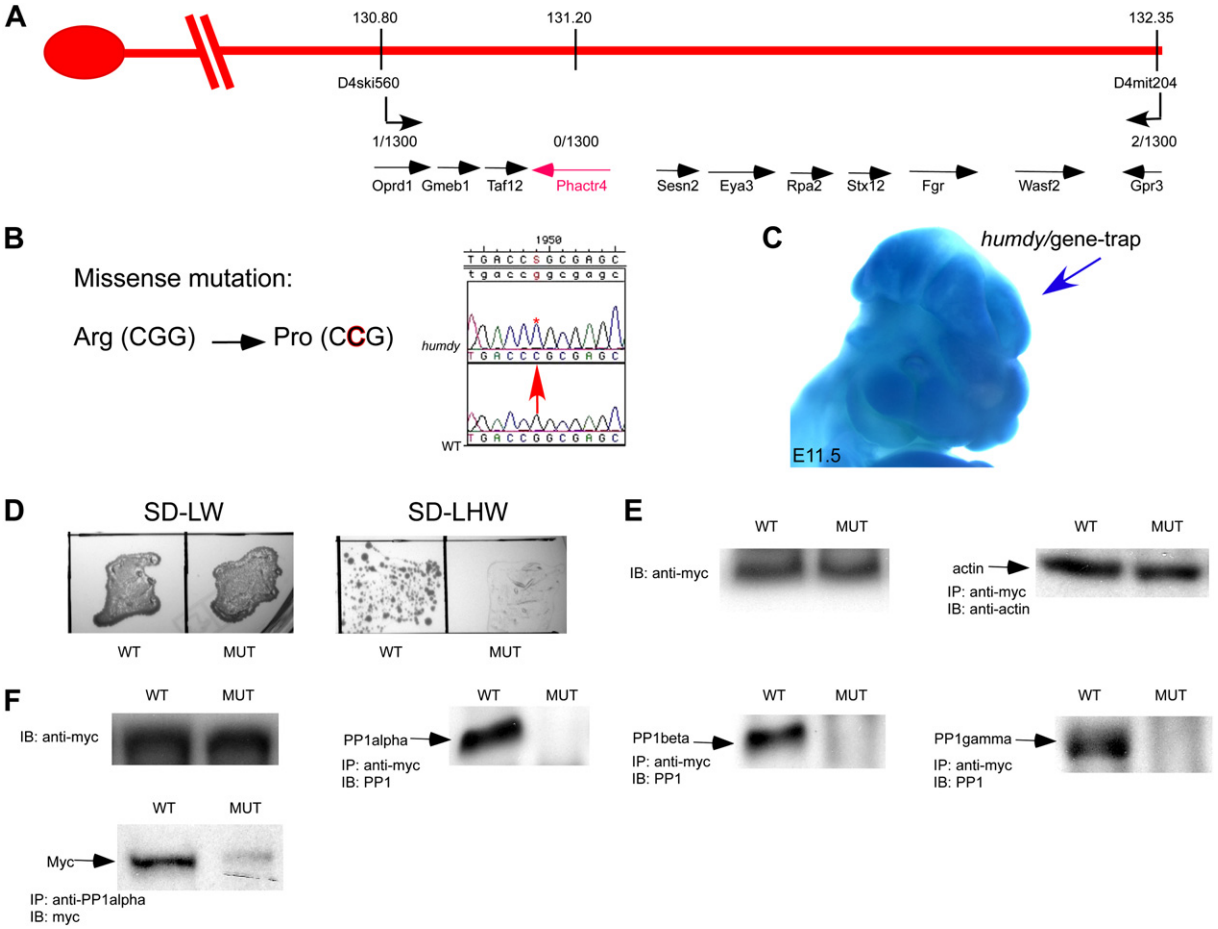

Figure 4. The *humdy* Gene Encodes *Phactr4*, and the *phactr4*^{humdy} Mutation Disrupts Interaction with PPI but Not Actin

(A) Genetic map of the *humdy* interval on mouse chromosome 4. Polymorphic markers and number of recombination events based on carriers are shown.

(B) Missense mutation from G to C resulting in Arg-to-Pro amino acid change in the conserved C terminus of the *Phactr4* gene.

(C) The gene-trap *phactr4* allele fails to complement the *phactr4*^{humdy} allele (arrow indicates exencephaly).

(D) Yeast two-hybrid assay. Yeast cells cotransfected with PP1-GAL4 DNA-binding domain and either wild-type or *humdy* mutation GAL4 activation domain and selected on minus leucine and tryptophan medium (SD-LW). Selection for interaction on medium lacking histidine (SD-LHW).

(E and F) Interaction of Phactr4 with endogenous actin and PP1. Immunoprecipitation with anti-Myc beads of wild-type Phactr4 or Phactr4^{humdy} followed by western blot analysis with anti-actin (E) or anti-PP1α, β, γ ([F], top row) antibodies. Immunoprecipitation with anti-PP1α followed by western blot analysis with anti-Myc antibody to detect interaction with wild-type Phactr4 or Phactr4^{humdy} ([F], lower row). Phactr4^{humdy} binds actin, but binding to all PP1 proteins is severely disrupted.

Phactr4 is also expressed in the neural retina and lens (Figures 5F and 5H).

Subcellular Localization of Phactr4, F-Actin, and PP1 in the Embryonic Neural Tube

Phactr1 is localized in the cytoplasm, whereas Phactr3 is in the nucleus (Allen et al., 2004; Sagara et al., 2003). To determine the in vivo subcellular localization of Phactr4, we used our polyclonal antibody to Phactr4: specificity shown by western blot of E10.5 embryo lysates and immunohistochemistry of E12.5 eye (Figures 5G–5I). Immunohistochemistry on E9.5 wild-type cranial neural tube showed Phactr4 was strongly expressed in the cytoplasm but not the nucleus (Figure 5J), similar to subcellular localization of Phactr1 (data not shown). Phactr4 also colocalized with F-actin (Figures 5J–5L), consistent with its ability to bind actin by coimmunoprecipitation. In the *humdy* neural tube, the mutant protein is still expressed and localized to the cytoplasm (Figure 5M), in accord with its retained ability to bind actin. In wild-type, PP1 is localized more strongly in the cytoplasm than in the nucleus (Figure 5N). However, in the *humdy* neural tube there was a slight but consistent shift in PP1 localization to the nucleus, as assayed by immunohistochemistry (Figure 5O) and nuclear/cytoplasmic fractionation (Figure 5S). Phactr1 binds at least PP1α, and Phactr1 is localized to the cytoplasm and expressed in neural tissue similarly to Phactr4. Redundancy between Phactr family members may explain why PP1 localization is not dramatically shifted in *humdy* mutants and why abnormal

proliferation occurs specifically in the hindbrain and retina of *humdy* embryos, although Phactr4 is expressed more broadly in the central nervous system. To explore further the ability of Phactr4 to affect subcellular localization of PP1, a gain-of-function study was performed by transfecting Myc-tagged wild-type *Phactr4* into HeLa cells. In untransfected cells, PP1 predominantly localized to the nucleus (Figure 5P), whereas in transfected cells there was a shift of PP1 into the cytoplasm (Figures 5Q and 5R). These loss- and gain-of-function experiments support the idea that Phactr4 binds PP1 and retains it in the cytoplasm, where Phactr4 protein is normally localized. Taken together with our data on a biochemical interaction between Phactr4 and PP1 (Figures 4D and 4F), this indicates a functional interaction between cytoplasmic PP1 and Phactr4 within the embryonic neural tube, the tissue affected in *humdy* mutants.

Inhibitory Phosphorylation of PP1 Is Abnormally Increased in *phactr4*$^{humdy/humdy}$ Neural Tube and Retina

Abnormal cell-cycle regulation in *humdy* mutant neural tube and retina and disruption in PP1 binding suggested PP1 activity might be defective in *humdy* embryos. PP1 activity with respect to Rb and the cell cycle is regulated by an inhibitory phosphorylation (T320) on PP1 (Berndt et al., 1997). Thus, we examined inhibitory phosphorylation of PP1 using an anti-PT320PP1 antibody in vivo. First, we found PP1 T320 phosphorylation is spatially regulated in the E9.5 wild-type neural tube with more cells expressing phospho-T320PP1 dorsally (Figure 6A), in accord with differential proliferation at this stage. Second, in *humdy* E9.5 ventral neural tube and E12.5 neural retina, PP1 T320 phosphorylation was abnormally increased compared to wild-type (Figures 2Q, 2S, 6A, and 6B), corresponding to regions of misregulated proliferation. Thus, Phactr4 interaction with PP1 is required in vivo to regulate the state of inhibitory phosphorylation of PP1 and hence PP1 activity with regard to cell-cycle regulation.

Rb Is Abnormally Phosphorylated and E2F Target Expression Is Abnormally Increased in *phactr4*$^{humdy/humdy}$ Neural Tube and Retina

In terms of cell-cycle regulation, in vitro studies have shown that all three isoforms of PP1 interact with and dephosphorylate Rb (Vietri et al., 2006; Rubin et al., 2001). PP1 regulates Rb-mediated cell-cycle arrest and control at the G1/S transition by dephosphorylating and activating Rb (Ceulemans and Bollen, 2004). Phosphorylation of T320 of PP1 inhibits its phosphatase activity so that PP1 can no longer dephosphorylate Rb. Consequently, hyperphosphorylated Rb is unable to inhibit cell-cycle progression. The abnormal S phase entry defects in *humdy* embryos (Figures 1P, 1T, 1X, and 3K) and disruption in PP1 activity (Figures 2S and 6B) suggested dephosphorylation of Rb might be defective. We therefore examined Rb phosphorylation at S608 and S807/811, as phosphorylation of these sites inactivates Rb and leads to cell-cycle progression. Phosphorylation of these sites was abnormally increased in the *humdy* ventral neural tube at E9.5 and was present more broadly at E10.5 (Figures 6C–6F), correlating with increased Ki67-positive neuronal progenitors (Figures 1O, 1P, 1S, and 1T). In the *humdy* retina, the number of neural progenitors expressing phospho-S608Rb was also increased relative to wild-type (Figure 2R), and this corresponded to cells in which PP1 was phosphorylated and inhibited (Figures 2S and 2T). Thus, mutation of the PP1 binding site in Phactr4 results in decreased PP1 phosphatase activity and increased Rb phosphorylation at key regulatory serines in vivo.

Growth suppression by Rb is achieved by its ability to bind E2F and histone deacetylase and repress E2F target genes required for cell-cycle progression (Cobrinik, 2005; Dimova and Dyson, 2005). E2F binds primarily to the spacer region of Rb, but binding also seems to require the C terminus of Rb (Adams, 2001). Phosphorylation at the spacer or C terminus disrupts Rb/E2F complexes, leading to derepression of E2F activity (Brown et al., 1999). Thus, we examined whether an E2F target was abnormally regulated in *humdy* mutants using anti-MCM2 antibody. Indeed, MCM2 was increased and expressed more broadly in *humdy* neural tube and retina (Figures 2U, 2V, 6G, and 6H), similar to disruption of the cell cycle and excess proliferation.

humdy Phenotype and Proliferation Defect Are Rescued by Loss of *E2f1*

Next, we undertook a genetic experiment to conclusively demonstrate that the primary defect in *humdy* mutants is due to misregulation of the cell cycle through abnormally increased E2F activity. The hypothesis is, if Phactr4-PP1 defects are due to misregulated E2F activity, then a decrease in E2F function should allow more normal development. We tested E2F1, as cell-cycle defects in the central nervous system of *Rb*$^{-/-}$ mice can be rescued by loss of *E2f1* (Tsai et al., 1998). Dramatically, *phactr4*$^{humdy/humdy}$*; E2f1*$^{-/-}$ embryos are rescued, as evidenced by complete (n = 3/5) or partial (n = 2/5) rescue of exencephaly and by essentially wild-type expression of markers of proliferation and differentiation within the cranial neural tube (Figures 6I–6L; compare with Figures 1S, 1T, 1Y, 1Z, 3J, and 3K), as well as MCM2 expression (compare Figure 6O to Figures 6G and 6H). Even more intriguingly, loss of one allele of *E2f1* is sufficient to completely rescue exencephaly (Figures 6M and 6N; 7 complete rescue, 6 partial rescue of 13 total). Coloboma is also rescued by loss of *E2f1* (data not shown). Thus, although it was possible that Phactr4 and PP1 could have other critical targets in the defective tissues, this rescue provides very strong genetic and functional evidence that the key target of Phactr4 during neurulation and eye development is the cell cycle through its regulator E2F1.

DISCUSSION

Here we identify a mutation in mouse *Phactr4* that specifically disrupts PP1 binding, leading to an inhibitory phosphorylation of PP1. This decreases the ability of PP1 to

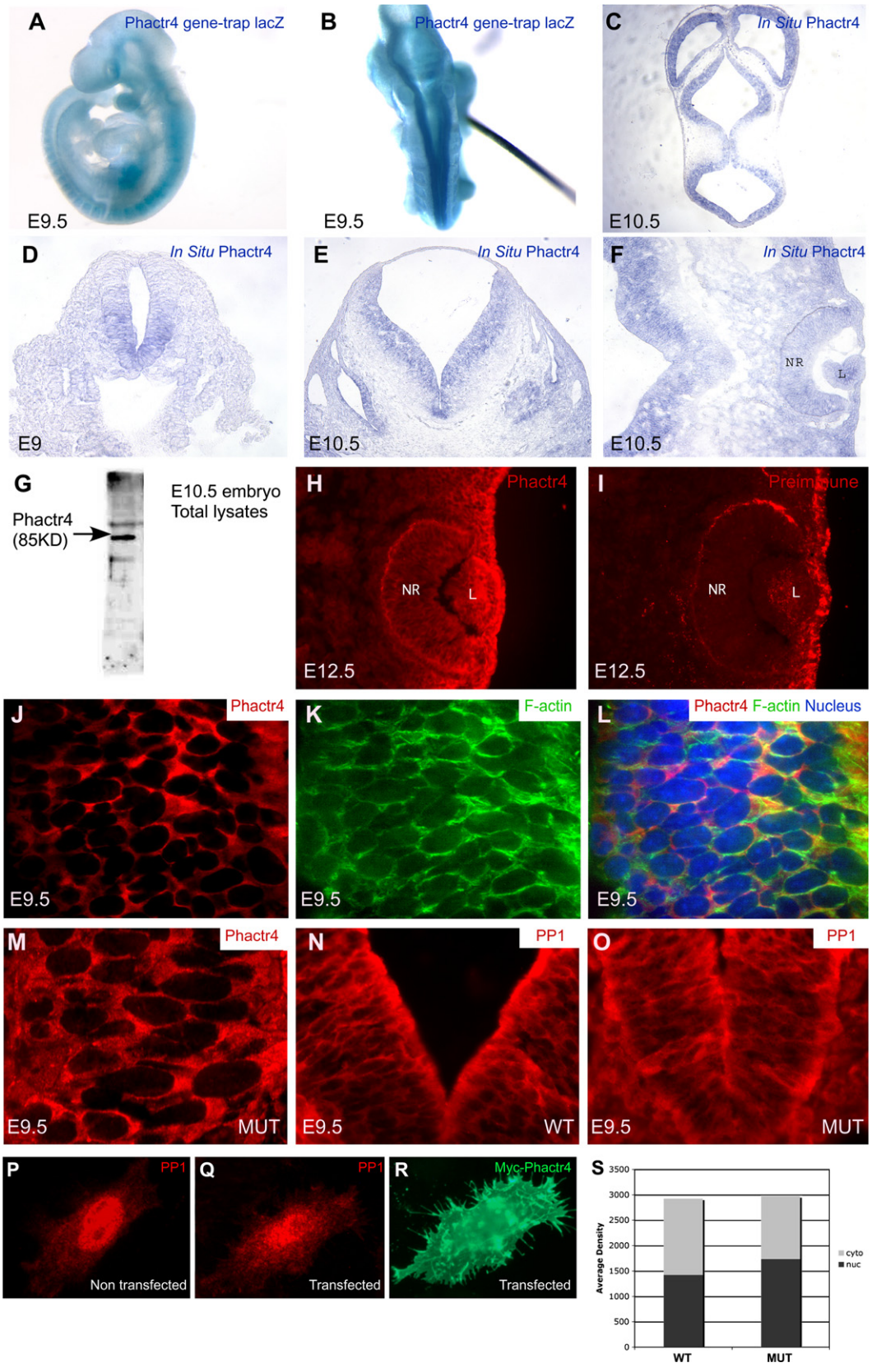
A
Phactr4 gene-trap lacZ
E9.5
B
Phactr4 gene-trap lacZ
E9.5
C
In Situ Phactr4
E10.5
D
In Situ Phactr4
E9
E
In Situ Phactr4
E10.5
F
In Situ Phactr4
NR
L
E10.5
G
Phactr4
(85KD)
E10.5 embryo
Total lysates
H
Phactr4
NR
L
E12.5
I
Preimmune
NR
L
E12.5
J
Phactr4
E9.5
K
F-actin
E9.5
L
Phactr4 F-actin Nucleus
E9.5
M
Phactr4
E9.5
MUT
N
PP1
E9.5
WT
O
PP1
E9.5
MUT
P
PP1
Non transfected
Q
PP1
Transfected
R
Myc-Phactr4
Transfected
S
Average Density
3500
3000
2500
2000
1500
1000
500
0
WT
MUT
cyto
nuc

dephosphorylate and activate Rb and leads to abnormal E2F activity and dramatically increased proliferation within the cranial neural tissue and the neural retina, causing exencephaly and retinal coloboma. The *humdy* phenotypes are rescued by loss of *E2f1* function, hence establishing a genetic and biochemical pathway from Phactr4 to direct control of the cell cycle during critical aspects of embryogenesis.

Phactr4 Controls Cell-Cycle Progression by Regulating Rb and E2F1 Function

humdy mutants display exencephaly and coloboma and severe cell-cycle defects: a shortened cell cycle, an inability of cells to properly exit the cell cycle, a substantial increase in the ratio of proliferating to differentiated cells, and increased neurogenesis at later stages. The dramatic rescue of the *humdy* phenotype by loss of *E2f1*, even a single allele, is particularly intriguing, as *E2f1*$^{-/-}$ mice are viable and fertile and hence only upon mutation of *Phactr4* is a strong requirement for E2F1 in regulation of the in vivo cell cycle revealed. These studies conclusively show that disruption of the cell cycle leads to the morphological and molecular defects observed in *humdy* mutants.

Our data support and provide in vivo evidence for a connection between PP1 and control of Rb phosphorylation. To further tie this pathway together, we showed the *phactr4* phenotypes are rescued by loss of *E2f1*. Rb is the best-known regulator of E2F1 function and, indeed, we found Rb is normally hypophosphorylated in the ventral neural tube at E9.5 and this spatial regulation is disrupted in *humdy* mutants. In the wild-type E9.5 neural tube, there is complete concordance between the domain of *Phactr4* expression in the ventral neural tube with active PP1 and hypophosphorylated Rb. In the E9.5 *humdy* ventral neural tube, PP1 function is inhibited and Rb is hyperphosphorylated. A day later, after neural closure, *Phactr4* is normally expressed throughout the ventricular zone of the cranial neural tube, and in *humdy* mutants, Rb is hyperphosphorylated throughout the expanded ventricular zone. This later defect in Rb phosphorylation could be a secondary consequence of the misregulated cell cycle. However, the earlier defect in Rb phosphorylation is highly correlated to the pattern of *Phactr4* and PP1 activity and therefore is likely a primary defect. In the *humdy* eye, we also established a tight correlation between PP1 inactivation and Rb hyperphosphorylation. In both the *humdy* neural tissue and eye, we observe ectopic transcription of the E2F target, MCM2, and abnormal cell-cycle progression at the G1/S transition, and these defects are rescued by loss of *E2f1*, a direct target of Rb. Thus, loss of the upstream regulator of Rb (Phactr4) is compensated for by loss of the downstream effector of Rb (E2F1), allowing normal neural and eye development.

Phactr4 localizes to the cytoplasm in both wild-type and *humdy* mutants, most likely through its binding to the actin cytoskeleton. One model for Phactr4 function is that Phactr4 helps retain PP1 in the cytoplasm, through association of Phactr4 with the actin cytoskeleton. Indeed, loss- and gain-of-function studies show Phactr4 regulates the cytoplasmic/nuclear distribution of PP1. We propose that during the G1 phase, PP1 translocates to the nucleus in a regulated manner, where it dephosphorylates and activates Rb as well as perhaps other cell-cycle regulators. In the *humdy* neural tube and retina, Phactr4 no longer binds PP1, which allows free PP1 to translocate into the nucleus in an unregulated manner and become inactivated by nuclear inhibitors, leading to abnormal cell-cycle progression in *humdy* embryos.

However, *humdy* mutant cell-cycle defects and embryonic phenotypes are more severe than those in *Rb* null embryos. An intriguing possibility for the more severe defect is that Phactr4 may control the activity of multiple regulators of cell-cycle progression: both Rb-dependent and Rb-independent pathways. One possibility is that Phactr4 controls activity of the Rb gene family: Rb, p107, and p130. Future experiments are required to determine whether the Rb family as a whole is regulated by Phactr4. The Rb family proteins have structural similarities in the pocket region important for binding to E2F family members (Mulligan and Jacks, 1998), and genetic interaction studies between Rb family members in mice suggest redundant roles. Indeed, some of the *phactr4* phenotypes are similar to *Rb* or *Rb* family double or triple mutants. *Rb/p107* double knockout embryos die earlier in embryogenesis than single knockouts and with more severe cell-cycle defects (Lee et al., 1996). Embryonic fibroblasts deficient in *Rb/p107/p130* show a shorter cell

Figure 5. *Phactr4* Gene Expression and Subcellular Localization of Phactr4 and PP1

(A and B) Whole-mount *LacZ* staining of *Phactr4*$^{+/gene\text{-}trap}$ embryos.

(C–F) Section in situ of wild-type embryos with antisense probe for *Phactr4* showing strong expression in neural tube and neural retina (NR; L, lens).

(D and E) *Phactr4* is expressed dynamically, first in the ventral neural tube during neurulation stage E9 (D), then ubiquitously throughout the dorsoventral neural tube at E10.5 ([E]; dorsal at top in [D] and [E]).

(G) Western blot of E10.5 wild-type embryo lysate detected with anti-Phactr4 antibody.

(H and I) Immunofluorescence of E12.5 wild-type eye detected with anti-Phactr4 antibody (H) or preimmune serum (I).

(J–M) Confocal images (100×) showing subcellular localization of Phactr4 and F-actin in wild-type (J–L) and *humdy* (M) neural tube at E9.5. Nucleus is visualized with DAPI. Phactr4 is strongly localized in the cytoplasm, where it colocalizes with F-actin, but not the nucleus, and is properly localized in the *humdy* mutant.

(N and O) Cross-sections of E9.5 ventral neural tube with PP1α immunostaining. PP1 is expressed strongly in the cytoplasm and more weakly in the nucleus of wild-type embryos, and localization is slightly shifted to the nucleus in *humdy* embryos.

(P–R) Immunofluorescence of HeLa cells with PP1α (red) and Myc staining (green). (P) Nontransfected cell.

(Q and R) Myc-tagged wild-type *Phactr4* transfected cell.

(S) Nuclear/cytoplasmic fractionation showing subtle but consistent shift of PP1 to the nucleus in *humdy* neural tube.

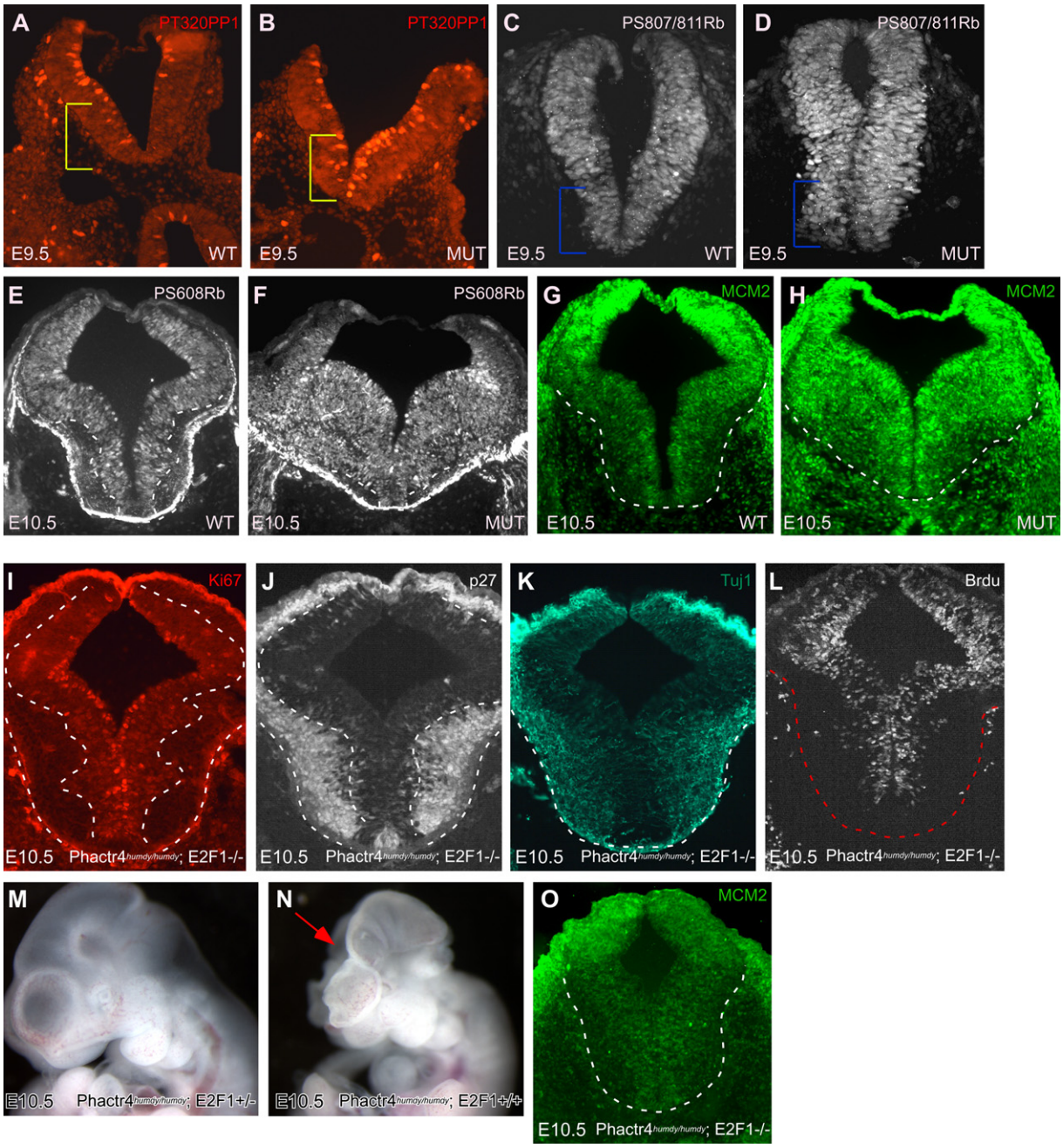

Figure 6. Abnormal Phosphorylation of PP1 and Rb in *humdy* Neural Tube and Rescue of Proliferation Defect in *phactr4*$^{humdy/humdy}$ by Loss of *E2f1*

(A–H) Cross-sections of wild-type (WT) and *humdy* (MUT) neural tube detected with anti-PT320PP1 (A and B), anti-phospho-specific Rb (C–F), or anti-MCM2 (G and H) antibodies.

(I–L and O) Cross-sections of cranial neural tube of *phactr4*$^{humdy/humdy}$; *E2f1*$^{-/-}$ embryos stained with anti-Ki67 (I), -p27 (J), -TuJ1 (K), -BrdU (L), and -MCM2 (O) antibodies. Defects of proliferation, differentiation, and E2F target expression in *humdy* embryos are rescued by loss of *E2f1* and are comparable to wild-type (see Figures 1, 6G, and 6H).

(M and N) Lateral views of rescued *phactr4*$^{humdy/humdy}$; *E2f1*$^{+/-}$ (M) and exencephalic (arrow) *phactr4*$^{humdy/humdy}$; *E2f1*$^{+/+}$ (N) embryos. Embryonic age is indicated in each panel.

cycle than wild-type or single or double mutant cells (Dannenberg et al., 2000; Sage et al., 2000), consistent with the shortened cell cycle in *humdy* neural tube. *Rb*-deficient cortical progenitor cells show a significant delay in terminal differentiation and enhanced neurogenesis (Callaghan et al., 1999; Ferguson et al., 2002), and *p107* regulates

neural progenitors in the embryonic and adult brain (Vanderluit et al., 2004). The *humdy* mutation affects early neural progenitors and causes a delay in differentiation with subsequently increased neurogenesis. Although it has been reported that *Rb* is not present in retinal progenitors in the later embryonic eye (Spencer et al., 2005), it is of note that we observed phosphorylated and unphosphorylated forms of Rb in retinal progenitors at E12.5 and that Rb is detected in P0 retinal progenitors (Zhang et al., 2004). *Rb* loss in the brain and retina, or loss of *Rb* and *p107* in the retina, causes ectopic division of differentiating cells (Chen et al., 2004; Ferguson et al., 2002; MacPherson et al., 2004). This is consistent with the ectopic division seen in the *humdy* neural tube and retina, although this cell-cycle exit defect is more subtle in the *humdy* retina compared to *Rb* knockout. It must also be borne in mind that Phactr4 controls only the phosphorylation status of Rb, not *Rb* gene or protein levels, and hence is different from *Rb* loss. Therefore, it should not be assumed that the phenotypes would be the same for an *Rb* hyperphosphorylation mutant versus an *Rb* null.

The second possibility is that Phactr4 acts through Rb-independent pathways to regulate E2F1 activity. PP1 function in cell-cycle regulation is best studied through Rb regulation, and the majority of genetic and physiological evidence favors the view that the Rb family is the most important regulator of E2F1. However, it is possible that Phactr4-modulated PP1 activity could target other cell-cycle regulators to control E2F1 function. For example, cell-cycle kinases such as ATM/ATR and Chk1/2 can phosphorylate and positively regulate E2F1 activity (Lin et al., 2001; Stevens and La Thangue, 2003; Urist et al., 2004). Although PP1 has not been specifically implicated in dephosphorylation of any E2F family members, it is possible that reduced PP1 activity in *humdy* mutants could increase E2F1 activity, independently of Rb. Phactr4-PP1 could also indirectly affect E2F1 activity by altering the phosphorylation state and hence activity of cell-cycle kinases like cyclinA/CDK2 and JNK (Kishore et al., 2003; Krek and DeCaprio, 1995; Wang et al., 1999; Xu et al., 1994). For instance, CDC25 is an enzyme that phosphorylates cell-cycle kinases and is also a target of PP1. CDC25 is activated by PP1 and is an activator of mitotic entry (Margolis et al., 2003; Rudolph, 2007). However, the *humdy* phenotype is opposite of what might be expected, as PP1 function is inhibited in *humdy* mutants, which should lead to inhibition of CDC25 activity and a defect in mitotic entry, rather than acceleration of the cell cycle.

Many future experiments will be required to distinguish the Rb-dependent and Rb-independent regulation of E2F1 activity, and to determine the full range of Phactr4 functions and in vivo targets. The *phactr4*^{humdy} missense mutation in the PP1 binding site provides novel insight into the critical control of embryonic cell-cycle regulation and highlights another important in vivo role for Phactr4 in providing PP1, a phosphatase with a broad range of targets, specificity for its target Rb, as well as perhaps other critical cell-cycle regulators.

Model for Phactr4 Function in Temporal and Spatial Regulation of Proliferation in the Neural Tube and Retina

Our studies also highlight the interesting conclusion that Phactr4 controls a temporal and spatial specific transition in proliferation. Figure 7 presents a model that incorporates the restricted pattern of *Phactr4* expression at the time of cranial neural tube closure, the regionally regulated proliferation, and the phosphorylation state of PP1 and Rb in the ventral and dorsal halves of wild-type and *humdy* mutant neural tubes.

In wild-type embryos at the time of neural tube closure, *Phactr4* expression is strongest in the ventral neural tube. There is differential proliferation, with more cells cycling in the dorsal half of the neural tube relative to the ventral half. Dorsally, more cells express a form of PP1 phosphorylated on an inhibitory site, which decreases PP1's phosphatase activity. There is a corresponding increase in hyperphosphorylated Rb, and this correlates with a higher rate of proliferation in the dorsal neural tube. In contrast, on the ventral half, *Phactr4* is expressed and available to bind PP1 and tether it in the cytoplasm through the binding of Phactr4 to actin. PP1 binding to Phactr4 retains PP1 in an active state, as it does not undergo inhibitory phosphorylation. Thus, during the cell cycle when PP1 shuttles to the nucleus of the ventral cells, it can dephosphorylate and activate Rb such that Rb can bind E2F and prevent cell-cycle progression.

In the *humdy* mutant at the time of neural closure, there is a significant increase in number of proliferating cells in the ventral neural tube. The *humdy* mutation does not affect Phactr4 protein expression or subcellular localization but specifically disrupts its ability to bind to PP1, and this leads to acquisition of an inhibitory phosphorylation on PP1. This decreases the ability of PP1 to dephosphorylate Rb, and hence Rb becomes hyperphosphorylated and can no longer bind E2F. This leads to abnormal activation of E2F targets and cell-cycle progression. Thus, loss of Phactr4 binding to PP1 results in misregulated proliferation in the ventral neural tube due to the ensuing cascade of E2F misregulation.

A day after neural tube closure, *Phactr4* expression is no longer restricted within the neural tube and instead is broadly expressed in both dorsal and ventral halves. In *humdy* mutants, there is now misregulated proliferation throughout the dorsoventral aspects of the neural tube at E10.5, followed by massive overgrowth of the neural tissue and increased neurogenesis. Phactr4 is required to regulate both cell-cycle length and exit from the cell cycle. *Phactr4* is also expressed in the eye, and this tissue is affected in the *humdy* mutant with similar misregulation of PP1 and Rb phosphorylation and abnormal proliferation. Therefore, our in vivo studies demonstrate the functional importance of Phactr4 in regulating embryonic proliferation in time and space.

Our studies conclusively show that the cell-cycle defect in *humdy* mutants is the cause of exencephaly, as neural tube closure and proliferation defects are rescued by loss of *E2f1*. Although closure of the neural tube and optic

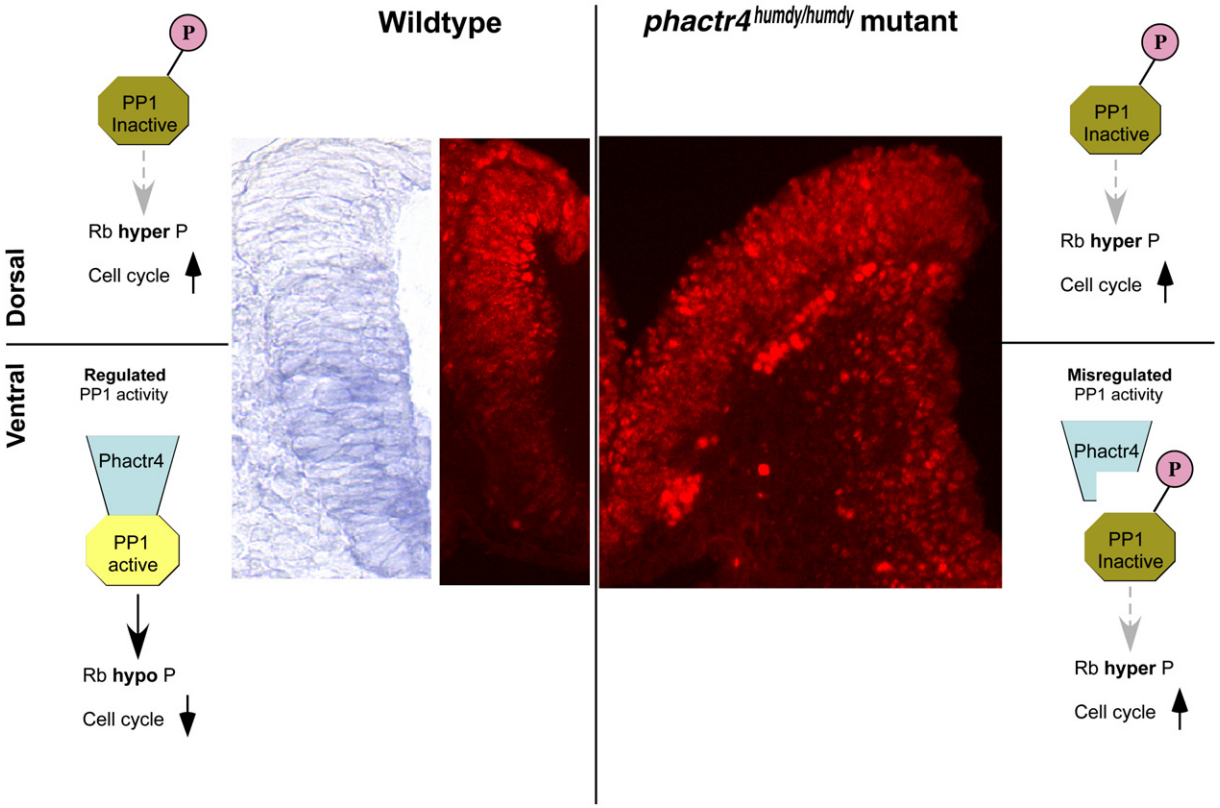

Figure 7. Model for Phactr4 Regulation of PP1 and Rb Activity in the Dorsal and Ventral Neural Tube during Neural Tube Closure
Phactr4 RNA is normally localized to the ventral neural tube at E9.5 in a region of reduced proliferation. The *phactr4*^{humdy} mutation causes abnormally increased proliferation in the ventral neural tube during neurulation. The Phactr4^{humdy} protein cannot bind PP1, and this leads to an inhibitory phosphorylation of PP1, decreased PP1 phosphatase activity, Rb hyperphosphorylation, and cell-cycle progression in the *phactr4*^{humdy} ventral neural tube.

fissure are very different processes, our data indicate that misregulated proliferation is also the cause of retinal coloboma in *humdy* mutants. Regionalized proliferation along the dorsoventral axis in the cranial neural tube at the time of closure has been noted but its importance has not been established (Copp et al., 2003). Our work provides what is, to our knowledge, the first identification of a molecular regulator of this differential proliferation. These studies therefore demonstrate that spatially regulated proliferation is necessary for cranial neural tube closure and that Phactr4 is a cell-cycle regulator specifically required for this controlled proliferation.

EXPERIMENTAL PROCEDURES

Mouse Strains, Genotyping, and *humdy* Mutation Identification

humdy was identified in a screen for recessive ENU-induced mutations that cause morphological abnormalities at E12.5 (Garcia-Garcia et al., 2005; Kasarskis et al., 1998; Zohn et al., 2005). The *humdy* mutation was induced with ethyl nitrosourea on a C57BL/6J genetic background and outcrossed to C3H3B/FeJ for more than ten generations to establish a congenic line. No phenotypic variation was observed on the different backgrounds. *humdy* was mapped between Massachusetts Institute of Technology (MIT) SSLP markers D4 mit203 and D4 mit204. For high-resolution mapping, additional markers were generated: D4ski4010L (5′-TGGTGGCAGCTCTTACTCCT-3′), D2ski4010R (5′-TTTGCTTACAAAGGGGGATG-3′), D4ski55-50L (5′-CAAGTGTA CCCATGCACACC-3′), and D4ski55-50R (5′-TCATGGCCAGTGAA GTGTTC-3′). The *humdy* mutation was identified by sequencing *Phactr4* cDNAs generated by RT-PCR (SuperScript One-Step RT-PCR; Invitrogen) using RNA from E10.5 *humdy/humdy* and C57BL/6J embryos. Mouse embryonic stem (ES) cell line RRA075 has a gene-trap insertion in *Phactr4* (http://baygenomics.ucsf.edu/). Mice were generated by blastocyst injection of RRA075 ES cells and kept on C3H background and genotyped by PCR with *lacZ* primers (Liu et al., 1999a) and/or MIT marker D4 mit204. Mice lacking *E2f1* were a gift from Dr. J. DeGregori.

Histology and RNA and Protein Localization and Quantification

β-galactosidase activity in whole-mount embryos from the gene-trap line was detected by X-gal staining (Eggenschwiler et al., 2001). Section RNA in situ hybridization (Holmes and Niswander, 2001) results were identical with digoxygenin-labeled probes from two regions of *Phactr4*. Antibody stainings on fixed frozen 10 μm sections of E8.5–E14.5 embryos (Timmer et al., 2002) used anti-Ki67 (Novocastra), anti-PH3, anti-cortactin (Upstate), anti-TuJ1 (Covance), anti-p27 (BD Biosciences), anti-F-actin (Chemicon), anti-PERM, anti-PS608Rb, anti-PS807/811Rb, anti-PT320 (Cell Signaling), and anti-MCM2 (Transduction Laboratories) antibodies. Anti-PP1α and anti-Phactr1 antibodies were kind gifts from Drs. P. Allen and P. Greengard. The anti-Phactr4 peptide (TTKTANDQREKTVSL) antibody was generated by Bio-Synthesis, Incorporated. BrdU (1 mg/20 g body weight; Sigma) was injected intraperitoneally 4 hr before sacrifice and detected with anti-BrdU antibody (Roche). For nuclear/cytoplasmic fractionation,

wild-type and *humdy* cranial regions were dissected, homogenized in hypotonic buffer with detergent and 1 mM DTT, and then processed as described in the Active Motif nuclear extract kit. Band intensity was quantified with the Bio-Rad Quantity One program.

Mitotic cell number (PH3-positive) was quantified in sections from E9.5 wild-type or *humdy* cranial neural tube and E12.5 retina. Using age-matched littermates and the Wilcoxon signed rank test, the average difference between wild-type and mutant dorsal neural tube was not significant (p value = 0.67), whereas in the *humdy* ventral neural tube there was a statistically significant (p = 0.046) increase in mitotic cells. The average difference between wild-type and mutant retina was 4.8 (p = 0.042). There was no difference between *humdy* dorsal versus ventral neural tube using the Mann-Whitney U test (nonparametric t test; p value = 0.936).

Cumulative BrdU Assay

Cumulative BrdU labeling in E10.5 embryos was performed by repeated intraperitoneal injections of BrdU into pregnant females at 2 hr intervals. Samples were fixed 30 min after injection and the time points were 30 min, 2 hr 30 min, 4 hr 30 min, 6 hr 30 min, and 8 hr 30 min, and six embryos (wild-type or mutant) per time point were analyzed. The proportion of BrdU-stained nuclei of neuroprogenitors was used to calculate Tc (total cell-cycle length) and Ts (S phase) using the Excel program kindly provided by Drs. R. Nowakowski and F. Calegari (Nowakowski et al., 1989).

Yeast Two-Hybrid Assays

Wild-type and *humdy* mutant *Phactr4* constructs were ligated into pPC86, a GAL4 activation domain fusion vector, and PP1α (a gift of Drs. P. Allen and P. Greengard) was ligated into pPC62, a GAL4 DNA-binding domain fusion vector. Yeast two-hybrid experiments were performed as per the Clontech Matchmaker Gal4 two-hybrid system.

Coimmunoprecipitation and Cell Cultures

Wild-type and *humdy* mutant *Phactr4* constructs were ligated into mammalian expression vector pCMV-Tag3 (Stratagene). HEK293T cells were transfected with plasmid DNA using Effectene transfection reagent (QIAGEN) and grown for at least 2 days. Transfected cells were lysed and total protein (1 mg) was used for immunoprecipitation (Allen et al., 2004) with anti-Myc (Cell Signaling), anti-actin, and anti-PP1α. HeLa cells were transfected with Myc-tagged wild-type *Phactr4* constructs and images were analyzed after staining with anti-Myc, anti-PP1α, anti-PP1β, and anti-PP1γ (Chemicon).

Supplemental Data

Supplemental Data include three figures and are available at http://www.developmentalcell.com/cgi/content/full/13/1/87/DC1/.

ACKNOWLEDGMENTS

We thank Audrey Greenfield, Patrick Allen, and Paul Greengard for generously providing reagents and advice to test Phactr4 interaction with PP1 and actin, Pengbo Zhou for insightful suggestions, and our lab members for help and comments throughout this project, in particular Aimin Liu, John Timmer, and Irene Zohn. We also thank Maria Barna, Kwangmin Choe, David Cobrinik, James DeGregori, Edward Espinoza, Davide Ruggero, and Hyungdon Ryoo for manuscript comments and the UCHSC Transgenic Core. This work was supported by NCI T32 CA86086 to J.G. and NIH U01 HD43478 to K.V.A. L.N. is an investigator of the Howard Hughes Medical Institute.

Received: April 10, 2006
Revised: February 20, 2007
Accepted: April 26, 2007
Published: July 2, 2007

REFERENCES

Adams, P.D. (2001). Regulation of the retinoblastoma tumor suppressor protein by cyclin/cdks. Biochim. Biophys. Acta *1471*, M123–M133.

Allen, P.B., Greenfield, A.T., Svenningsson, P., Haspeslagh, D.C., and Greengard, P. (2004). Phactrs 1–4: a family of protein phosphatase 1 and actin regulatory proteins. Proc. Natl. Acad. Sci. USA *101*, 7187–7192.

Axton, J.M., Dombradi, V., Cohen, P.T., and Glover, D.M. (1990). One of the protein phosphatase 1 isoenzymes in *Drosophila* is essential for mitosis. Cell *63*, 33–46.

Berndt, N. (2003). Roles and regulation of serine/threonine-specific protein phosphatases in the cell cycle. Prog. Cell Cycle Res. *5*, 497–510.

Berndt, N., Dohadwala, M., and Liu, C.W. (1997). Constitutively active protein phosphatase 1α causes Rb-dependent G1 arrest in human cancer cells. Curr. Biol. *7*, 375–386.

Booher, R.N., Alfa, C.E., Hyams, J.S., and Beach, D.H. (1989). The fission yeast cdc2/cdc13/suc1 protein kinase: regulation of catalytic activity and nuclear localization. Cell *58*, 485–497.

Brown, V.D., Phillips, R.A., and Gallie, B.L. (1999). Cumulative effect of phosphorylation of pRB on regulation of E2F activity. Mol. Cell. Biol. *19*, 3246–3256.

Callaghan, D.A., Dong, L., Callaghan, S.M., Hou, Y.X., Dagnino, L., and Slack, R.S. (1999). Neural precursor cells differentiating in the absence of Rb exhibit delayed terminal mitosis and deregulated E2F 1 and 3 activity. Dev. Biol. *207*, 257–270.

Ceulemans, H., and Bollen, M. (2004). Functional diversity of protein phosphatase-1, a cellular economizer and reset button. Physiol. Rev. *84*, 1–39.

Chen, D., Livne-bar, I., Vanderluit, J.L., Slack, R.S., Agochiya, M., and Bremner, R. (2004). Cell-specific effects of RB or RB/p107 loss on retinal development implicate an intrinsically death-resistant cell-of-origin in retinoblastoma. Cancer Cell *5*, 539–551.

Chow, R.L., and Lang, R.A. (2001). Early eye development in vertebrates. Annu. Rev. Cell Dev. Biol. *17*, 255–296.

Cobrinik, D. (2005). Pocket proteins and cell cycle control. Oncogene *24*, 2796–2809.

Cohen, P.T. (2002). Protein phosphatase 1—targeted in many directions. J. Cell Sci. *115*, 241–256.

Colas, J.F., and Schoenwolf, G.C. (2001). Towards a cellular and molecular understanding of neurulation. Dev. Dyn. *221*, 117–145.

Copp, A.J., Greene, N.D., and Murdoch, J.N. (2003). The genetic basis of mammalian neurulation. Nat. Rev. Genet. *4*, 784–793.

Dannenberg, J.H., van Rossum, A., Schuijff, L., and te Riele, H. (2000). Ablation of the retinoblastoma gene family deregulates G(1) control causing immortalization and increased cell turnover under growth-restricting conditions. Genes Dev. *14*, 3051–3064.

Dimova, D.K., and Dyson, N.J. (2005). The E2F transcriptional network: old acquaintances with new faces. Oncogene *24*, 2810–2826.

Doonan, J.H., and Morris, N.R. (1989). The bimG gene of *Aspergillus nidulans*, required for completion of anaphase, encodes a homolog of mammalian phosphoprotein phosphatase 1. Cell *57*, 987–996.

Durfee, T., Becherer, K., Chen, P.L., Yeh, S.H., Yang, Y., Kilburn, A.E., Lee, W.H., and Elledge, S.J. (1993). The retinoblastoma protein associates with the protein phosphatase type 1 catalytic subunit. Genes Dev. *7*, 555–569.

Eggenschwiler, J.T., Espinoza, E., and Anderson, K.V. (2001). Rab23 is an essential negative regulator of the mouse Sonic hedgehog signalling pathway. Nature *412*, 194–198.

Ferguson, K.L., Vanderluit, J.L., Hebert, J.M., McIntosh, W.C., Tibbo, E., MacLaurin, J.G., Park, D.S., Wallace, V.A., Vooijs, M., McConnell, S.K., and Slack, R.S. (2002). Telencephalon-specific Rb knockouts

reveal enhanced neurogenesis, survival and abnormal cortical development. EMBO J. *21*, 3337–3346.

Garcia-Garcia, M.J., Eggenschwiler, J.T., Caspary, T., Alcorn, H.L., Wyler, M.R., Huangfu, D., Rakeman, A.S., Lee, J.D., Feinberg, E.H., Timmer, J.R., and Anderson, K.V. (2005). Analysis of mouse embryonic patterning and morphogenesis by forward genetics. Proc. Natl. Acad. Sci. USA *102*, 5913–5919.

Gowen, L.C., Johnson, B.L., Latour, A.M., Sulik, K.K., and Koller, B.H. (1996). Brca1 deficiency results in early embryonic lethality characterized by neuroepithelial abnormalities. Nat. Genet. *12*, 191–194.

Holmes, G., and Niswander, L. (2001). Expression of slit-2 and slit-3 during chick development. Dev. Dyn. *222*, 301–307.

Juriloff, D.M., and Harris, M.J. (2000). Mouse models for neural tube closure defects. Hum. Mol. Genet. *9*, 993–1000.

Kasarskis, A., Manova, K., and Anderson, K.V. (1998). A phenotype-based screen for embryonic lethal mutations in the mouse. Proc. Natl. Acad. Sci. USA *95*, 7485–7490.

Kim, J.K., Huh, S.O., Choi, H., Lee, K.S., Shin, D., Lee, C., Nam, J.S., Kim, H., Chung, H., Lee, H.W., et al. (2001). Srg3, a mouse homolog of yeast SWI3, is essential for early embryogenesis and involved in brain development. Mol. Cell. Biol. *21*, 7787–7795.

Kishore, R., Luedemann, C., Bord, E., Goukassian, D., and Losordo, D.W. (2003). Tumor necrosis factor-mediated E2F1 suppression in endothelial cells: differential requirement of c-Jun N-terminal kinase and p38 mitogen-activated protein kinase signal transduction pathways. Circ. Res. *93*, 932–940.

Krek, W., and DeCaprio, J.A. (1995). Cell synchronization. Methods Enzymol. *254*, 114–124.

Lardelli, M., Williams, R., Mitsiadis, T., and Lendahl, U. (1996). Expression of the Notch 3 intracellular domain in mouse central nervous system progenitor cells is lethal and leads to disturbed neural tube development. Mech. Dev. *59*, 177–190.

Lee, M.H., Williams, B.O., Mulligan, G., Mukai, S., Bronson, R.T., Dyson, N., Harlow, E., and Jacks, T. (1996). Targeted disruption of p107: functional overlap between p107 and Rb. Genes Dev. *10*, 1621–1632.

Lin, W.C., Lin, F.T., and Nevins, J.R. (2001). Selective induction of E2F1 in response to DNA damage, mediated by ATM-dependent phosphorylation. Genes Dev. *15*, 1833–1844.

Liu, A., Losos, K., and Joyner, A.L. (1999a). FGF8 can activate Gbx2 and transform regions of the rostral mouse brain into a hindbrain fate. Development *126*, 4827–4838.

Liu, C.W., Wang, R.H., Dohadwala, M., Schonthal, A.H., Villa-Moruzzi, E., and Berndt, N. (1999b). Inhibitory phosphorylation of PP1α catalytic subunit during the G(1)/S transition. J. Biol. Chem. *274*, 29470–29475.

Ludlow, J.W., Glendening, C.L., Livingston, D.M., and DeCarprio, J.A. (1993). Specific enzymatic dephosphorylation of the retinoblastoma protein. Mol. Cell. Biol. *13*, 367–372.

MacPherson, D., Sage, J., Kim, T., Ho, D., McLaughlin, M.E., and Jacks, T. (2004). Cell type-specific effects of Rb deletion in the murine retina. Genes Dev. *18*, 1681–1694.

Margolis, S.S., Walsh, S., Weiser, D.C., Yoshida, M., Shenolikar, S., and Kornbluth, S. (2003). PP1 control of M phase entry exerted through 14-3-3-regulated Cdc25 dephosphorylation. EMBO J. *22*, 5734–5745.

Mulligan, G., and Jacks, T. (1998). The retinoblastoma gene family: cousins with overlapping interests. Trends Genet. *14*, 223–229.

Nowakowski, R.S., Lewin, S.B., and Miller, M.W. (1989). Bromodeoxyuridine immunohistochemical determination of the lengths of the cell cycle and the DNA-synthetic phase for an anatomically defined population. J. Neurocytol. *18*, 311–318.

Ohkura, H., Kinoshita, N., Miyatani, S., Toda, T., and Yanagida, M. (1989). The fission yeast dis2$^+$ gene required for chromosome disjoining encodes one of two putative type 1 protein phosphatases. Cell *57*, 997–1007.

Pagano, M., and Jackson, P.K. (2004). Wagging the dogma: tissue-specific cell cycle control in the mouse embryo. Cell *118*, 535–538.

Rubin, E., Mittnacht, S., Villa-Moruzzi, E., and Ludlow, J.W. (2001). Site-specific and temporally-regulated retinoblastoma protein dephosphorylation by protein phosphatase type 1. Oncogene *20*, 3776–3785.

Rudolph, J. (2007). Cdc25 phosphatases: structure, specificity, and mechanism. Biochemistry *46*, 3595–3604.

Sagara, J., Higuchi, T., Hattori, Y., Moriya, M., Sarvotham, H., Shima, H., Shirato, H., Kikuchi, K., and Taniguchi, S. (2003). Scapinin, a putative protein phosphatase-1 regulatory subunit associated with the nuclear nonchromatin structure. J. Biol. Chem. *278*, 45611–45619.

Sage, J., Mulligan, G.J., Attardi, L.D., Miller, A., Chen, S., Williams, B., Theodorou, E., and Jacks, T. (2000). Targeted disruption of the three Rb-related genes leads to loss of G(1) control and immortalization. Genes Dev. *14*, 3037–3050.

Sah, V.P., Attardi, L.D., Mulligan, G.J., Williams, B.O., Bronson, R.T., and Jacks, T. (1995). A subset of p53-deficient embryos exhibit exencephaly. Nat. Genet. *10*, 175–180.

Sherr, C.J., and Roberts, J.M. (2004). Living with or without cyclins and cyclin-dependent kinases. Genes Dev. *18*, 2699–2711.

Spencer, C., Pajovic, S., Devlin, H., Dinh, Q.D., Corson, T.W., and Gallie, B.L. (2005). Distinct patterns of expression of the RB gene family in mouse and human retina. Gene Expr. Patterns *5*, 687–694.

Stevens, C., and La Thangue, N.B. (2003). A new role for E2F-1 in checkpoint control. Cell Cycle *2*, 435–437.

Tamrakar, S., Rubin, E., and Ludlow, J.W. (2000). Role of pRB dephosphorylation in cell cycle regulation. Front. Biosci. *5*, D121–D137.

Timmer, J.R., Wang, C., and Niswander, L. (2002). BMP signaling patterns the dorsal and intermediate neural tube via regulation of homeobox and helix-loop-helix transcription factors. Development *129*, 2459–2472.

Tsai, K.Y., Hu, Y., Macleod, K.F., Crowley, D., Yamasaki, L., and Jacks, T. (1998). Mutation of E2f-1 suppresses apoptosis and inappropriate S phase entry and extends survival of Rb-deficient mouse embryos. Mol. Cell *2*, 293–304.

Urist, M., Tanaka, T., Poyurovsky, M.V., and Prives, C. (2004). p73 induction after DNA damage is regulated by checkpoint kinases Chk1 and Chk2. Genes Dev. *18*, 3041–3054.

Vanderluit, J.L., Ferguson, K.L., Nikoletopoulou, V., Parker, M., Ruzhynsky, V., Alexson, T., McNamara, S.M., Park, D.S., Rudnicki, M., and Slack, R.S. (2004). p107 regulates neural precursor cells in the mammalian brain. J. Cell Biol. *166*, 853–863.

Vietri, M., Bianchi, M., Ludlow, J.W., Mittnacht, S., and Villa-Moruzzi, E. (2006). Direct interaction between the catalytic subunit of protein phosphatase 1 and pRb. Cancer Cell Int. *6*, 3.

Wang, S., Nath, N., Minden, A., and Chellappan, S. (1999). Regulation of Rb and E2F by signal transduction cascades: divergent effects of JNK1 and p38 kinases. EMBO J. *18*, 1559–1570.

Weston, C.R., Wong, A., Hall, J.P., Goad, M.E., Flavell, R.A., and Davis, R.J. (2003). JNK initiates a cytokine cascade that causes Pax2 expression and closure of the optic fissure. Genes Dev. *17*, 1271–1280.

Xu, M., Sheppard, K.A., Peng, C.Y., Yee, A.S., and Piwnica-Worms, H. (1994). Cyclin A/CDK2 binds directly to E2F-1 and inhibits the DNA-binding activity of E2F-1/DP-1 by phosphorylation. Mol. Cell. Biol. *14*, 8420–8431.

Zhang, J., Gray, J., Wu, L., Leone, G., Rowan, S., Cepko, C.L., Zhu, X., Craft, C.M., and Dyer, M.A. (2004). Rb regulates proliferation and rod photoreceptor development in the mouse retina. Nat. Genet. *36*, 351–360.

Zohn, I.E., Anderson, K.V., and Niswander, L. (2005). Using genome-wide mutagenesis screens to identify the genes required for neural tube closure in the mouse. Birth Defects Res. A Clin. Mol. Teratol. *73*, 583–590.